592 J. Agric. Food Chem. 2011, 59, 592–600
DOI:10.1021/jf1032476

JOURNAL OF AGRICULTURAL AND FOOD CHEMISTRY
ARTICLE

Application of Artificial Neural Network (ANN) and Partial Least-Squares Regression (PLSR) to Predict the Changes of Anthocyanins, Ascorbic Acid, Total Phenols, Flavonoids, and Antioxidant Activity during Storage of Red Bayberry Juice Based on Fractal Analysis and Red, Green, and Blue (RGB) Intensity Values

Hong Zheng, Lingling Jiang, Heqiang Lou, Ya Hu, Xuecheng Kong, and Hongfei Lu*

College of Chemistry and Life Science, Zhejiang Normal University, Jinhua 321004, China

Artificial neural network (ANN) and partial least-squares regression (PLSR) models were developed to predict the changes of anthocyanin (AC), ascorbic acid (AA), total phenols (TP), total flavonoid (TF), and DPPH radical scavenging activity (SA) in bayberry juice during storage based on fractal analysis (FA) and red, green, and blue (RGB) intensity values. The results show the root mean squared error (RMSE) of ANN-FA decreased 2.44 and 12.45% for AC (RMSE = 18.673 mg/100 mL, R^2 = 0.939) and AA (RMSE = 8.694 mg/100 mL, R^2 = 0.935) compared with PLSR-RGB, respectively. In addition, PLSR-FA (RMSE = 5.966%, R^2 = 0.958) showed a 12.01% decrease in the RMSE compared with PLSR-RGB for predicting SA. For the prediction of TP and TF, however, both models showed poor performances based on FA and RGB. Therefore, ANN and PLSR combined with FA may be a potential method for quality evaluation of bayberry juice during processing, storage, and distribution, but the selection of the most adequate model is of great importance to predict different nutritional components.

KEYWORDS: Bayberry; anthocyanin; ascorbic acid; antioxidant activity; ANN; PLSR; fractal dimension

INTRODUCTION

Chinese bayberry (*Myrica rubra* Sieb. & Zucc.), an important economic Asian fruit crop belonging to the Myricaceae family, is a fruit with high nutritional components such as anthocyanins, carbohydrates, organic acids, flavonoids, and vitamins and is popular with local people (*1*). China is the major commercial production area for bayberry, and the annual output is about 300,000 tons (*2*). However, a key limitation to the commercial development of this fruit is its relatively short shelf life: it can be kept fresh for only 3 days at 20−22 °C and for 9−12 days at 0−2 °C (*3*), because it has no epicarp protection and ripens in the hot and rainy season of June−July. Although Wang et al. (*4*) and Yang et al. (*5*) applied methyl jasmonate and high-oxygen atmosphere to reduce fruit decay and improve the quality of Chinese bayberry fruit during storage, respectively, many fruits, to extend their consumption time, are usually processed into various products, especially bayberry juice. During storage, however, fruit juice usually undergoes a number of deteriorative reactions such as some nutrient degradation, microbial spoilage, development of off-flavor, and color changes, resulting in quality degradation of the product.

Recently, the nutritional quality of food during storage has become an increasingly important problem. Therefore, predicting the behavior of nutritional quality during the storage of foods by an accurate mathematic model is important. Several kinetics studies have been carried out to model nutrient changes in foods, such as anthocyanins (*6*, *7*), ascorbic acid (*8*, *9*), and lycopene (*10*). The Weibull distribution function as a new model has been used to describe chemical degradation kinetics of ascorbic acid in orange juice (*11*), antioxidant potential in fresh-cut watermelon (*12*), and anthocyanins in fresh-cut strawberries (*13*) during storage. In addition, many authors have proposed computer simulations to predict the quality degradation of foods during storage (*14*−*16*). Artificial neural networks (ANN) have the ability to model any linear or nonlinear relationship between the input and output data sets (*17*) and are widely applied in tasks involving economics (*18*), physics (*19*), engineering (*20*), geology (*21*), hydrology (*22*), etc. Recently, ANN also is an interesting method in several food-processing applications such as quality control (*23*), drying applications (*24*), thermal processing (*25*), and food freezing (*26*). Partial least-squares regression (PLSR) is a method for comparing two data sets by a linear multivariate model (*27*) and has been widely used as a calibration tool in chemometrics (*28*), QSAR (*29*), disease prediction (*30*), food research (*31*), etc. However, there have been no reports on modeling nutritional quality changes of bayberry juice using ANN and PLSR models based on fractal analysis (FA).

Food color is the first property that the consumer observes and has a remarkable influence on its acceptance. In the European Union, the color of food has been implemented in the quality

*Author to whom correspondence should be addressed (phone +86-0579-8228-2284; e-mail luhongfei63@yahoo.com.cn).

 Published on Web 12/29/2010

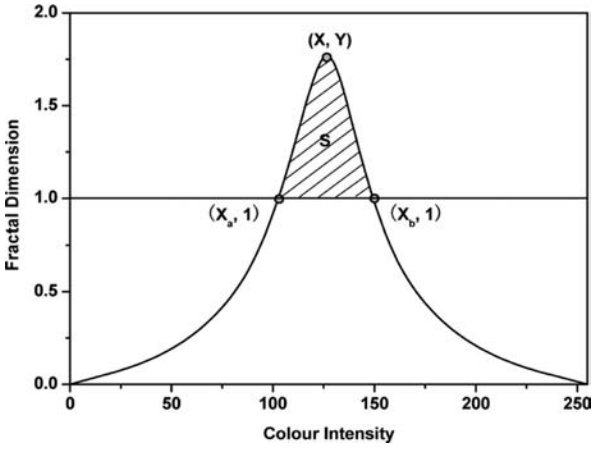

Figure 1. Graphical representation of the five fractal parameters calculated from the fractal spectrum of each color in this study: X_a, X_b, peak coordinates X and Y, and peak area S. The baseline with the fractal dimension $D = 1$ separates the fractal ($D > 1$) from the nonfractal ($D < 1$) zone of the spectrum.

control of the food industries (*32*). Tepper (*33*) also reported color retention of citrus juices is one of the parameters of its quality in the United States. Therefore, color changes of food materials during storage have been studied by many researchers (*34*−*36*). Fractals are mathematical sets that process high degrees of geometrical complexity and can model numerous natural phenomena (*37*). Fractal analysis has been successfully used in several areas such as materials science, geology, texture analysis, plant classification, and medical imaging (*38*−*42*). It has also been used to study structural and mechanical attributes of food materials (*43*). However, no information is available on using fractal measure of the color image to evaluate the quality of fruit juices during storage.

Therefore, the objectives of this research are (1) to evaluate the effectiveness of prediction of the changes of anthocyanin, ascorbic acid, total phenols, total flavonoid, and DPPH radical scavenging activity during storage of bayberry juice by means of fractal spectra traits originated from image analysis; (2) to compare the performance of prediction models based on fractal parameters and red, green, and blue (RGB) intensity values; and (3) to evaluate the performance derived by the use of ANN and PLSR models.

MATERIALS AND METHODS

Preparation of Bayberry Juice Samples. Fresh bayberries (*M. rubra* Sieb. & Zucc. cv. Biqi) were obtained from a local market in Jinghua (Zhejiang, China). The fruits were squeezed in a home juicer (Midea, JP351, China). Then the pulp−juice mixture of each fruit was filtered through a double layer of cheesecloth to remove the pulp. All juice samples were equally divided (25 mL) into 50 mL glass bottles (60 bottles) and pasteurized in a thermostatic water bath operating at 90 °C for 90 s before storage. After that, bayberry juices were rapidly cooled in an ice bath and were stored in a temperature-controlled storage locker at 25 °C in the dark for 12 days. About six bottles were selected at random to analyze each index every 2 days (0, 2, 4, 6, 8, 10, and 12) during storage.

Chemicals. 2,2′-Diphenyl-1-picrylhydrazyl (DPPH) free radical (purity ≥ 90%) and rutin (purity ≥ 95%) were of analytical grade and purchased from Sigma-Aldrich (St. Louis, MO). Gallic acid (purity ≥ 98%), ascorbic acid (purity ≥ 99%), Folin−Ciocalteu reagent (purity ≥ 99%), and 2,6-dichlorophenol indophenol (purity ≥ 99%) were purchased from Shanghai Sangon Biological Engineering Technology and Services Co., Ltd. (Shanghai, China).

Determination of Anthocyanin (AC) Content. The AC content of juices was determined with a modified pH differential method described by

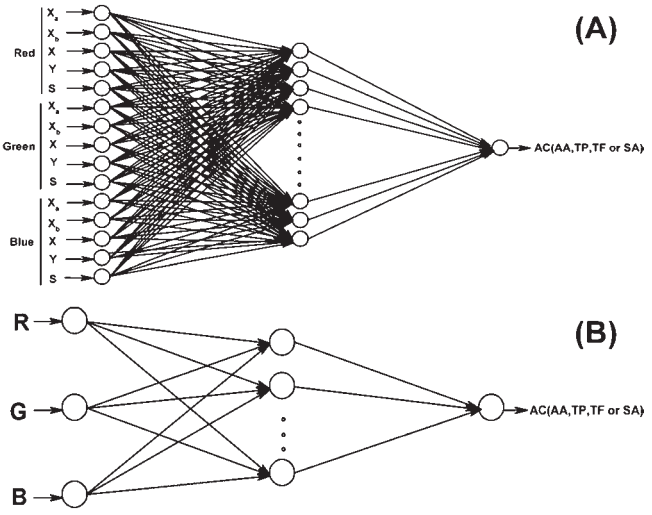

Figure 2. ANN model structure for predicting the changes of anthocyanins, ascorbic acid, total phenols, total flavonoids, and radical DPPH scavenging activity during storage of red bayberry juice based on fractal parameters (**A**) and RGB intensity values (**B**).

Meyers et al. (*44*), using two buffer systems: potassium chloride 0.025 M at pH 1.0 and sodium acetate 0.4 M at pH 4.5. Briefly, 1 mL of sample was transferred to a 10 mL volumetric flask and made up with each buffer. The absorbance of each equilibrated solution was then measured at 510 and 700 nm, using a UV−vis spectrophotometer. Quartz cuvettes of 1 cm path length were used, and all measurements were carried out at room temperature (25 °C). Absorbance readings were made against distilled water as a blank. The major anthocyanin is cyanidin-3-glucoside, which represents > 95% of the total anthocyanins in bayberry fruits (*45*). The AC content was calculated on the basis of cyanidin-3-glucoside (*46*) with a molecular weight of 445.2 g/mol and an extinction coefficient of 29600 L/mol·cm (*47*), as

$$\mathrm{AC} = [(A_{510} - A_{700})_{\mathrm{pH1.0}} - (A_{510} - A_{700})_{\mathrm{pH4.5}}] \times \mathrm{MW} \times \mathrm{DF} \times \frac{1000}{\varepsilon} \times L \quad (1)$$

where MW is the molecular weight of cyanidin-3-glucoside, DF is the dilution factor, L is the path length in cm, and ε is the molar extinction coefficient for cyanidin-3-glucoside. Results were expressed as milligram cyanidin-3-glucoside equivalents per 100 mL of juice.

Determination of Ascorbic Acid (AA) Content. The indophenol−xylene extraction method (*8*) for determination of AA content was performed by using a UV−vis spectrophotometer at a wavelength of 500 nm against xylene. Results of AA content were expressed as milligrams of ascorbic acid per 100 mL of juice. The AA content was measured in triplicate.

Determination of Total Phenolic (TP), Total Flavonoid (TF), and Radical DPPH Scavenging Activity (SA). In this study, TP and TF contents and SA were measured according to methods described in our earlier paper (*25*, *48*). The TP content in bayberry juice was determined using Folin−Ciocalteu reagent, the TF content was evaluated by a colorimetric assay method, and the SA value of juice was evaluated using the stable radical DPPH. The TP and TF contents were expressed as milligrams of GAE per 100 mL of juice and milligrams of rutin per 100 mL of juice, respectively, and the SA was the percentage of DPPH scavenging (%).

Image Acquisition and Fractal Spectrum. Bayberry juices were photographed using a Canon EOS 50D camera with a Canon EF-S 18−55 mm f/3.5−5.6 IS lens at 50 mm. The lighting for images was entirely from natural light on a sunny morning in the summer. All image acquisitions were carried out at least in triplicate. Fractal parameters were determined using fractal image analysis software (HarFA, Harmonic and Fractal Image Analyzer 5.4, freeware at http://www.fch.vutbr.cz/lectures/imagesci/) as described by Pandolfi et al. (*38*). The basic procedures were as follows: (i) each fruit color image was split in RGB color channels; (ii) each channel was

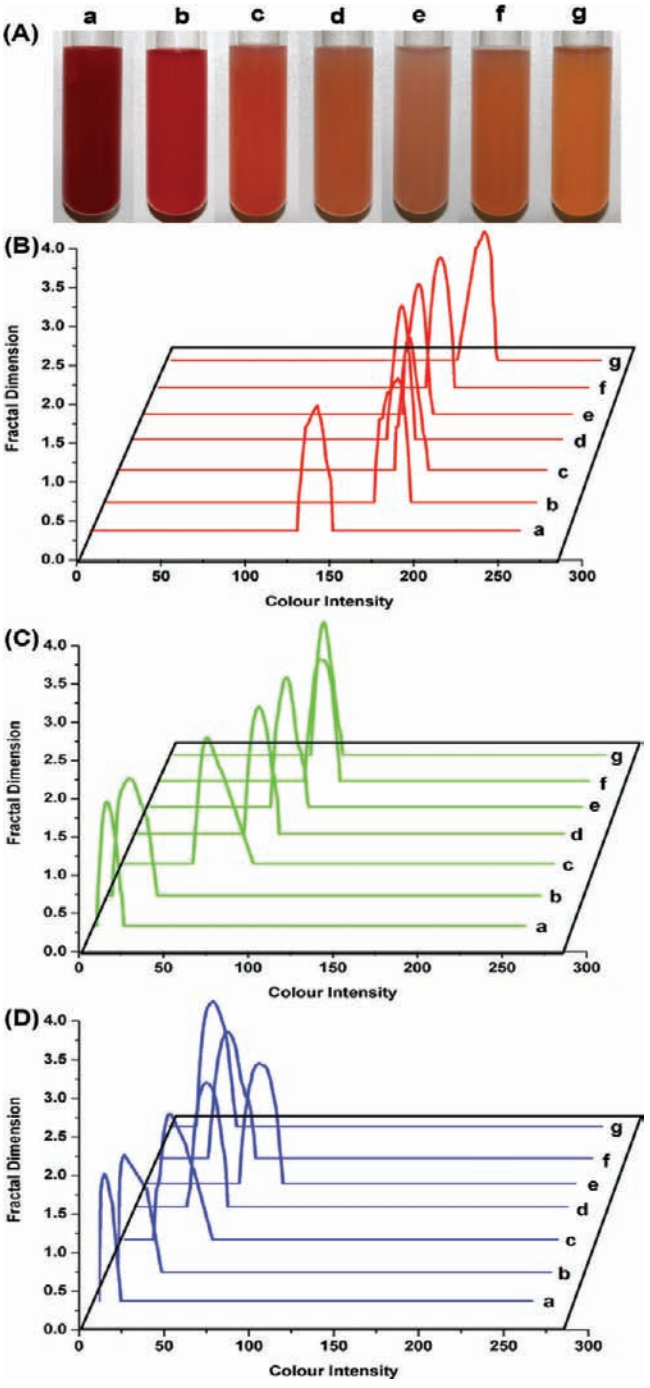

Figure 3. Changes of juice color (**A**) and fractal spectra of the red (**B**), green (**C**), and blue (**D**) channels derived from red bayberry juice during storage.

thresholded for a color value between 0 and 255; (iii) the fractal dimension (D) for each color channel was determined by the box counting method; (iv) then we got something called a "fractal spectrum", where fractal dimension is presented as a function of thresholding condition. After the baseline (D = 1) that separates the fractal (D >1) from the nonfractal (D <1) zone of the spectrum had been drawn, five fractal parameters (X_a, X_b, X, Y, and S) for each channel were calculated by OriginLab (OriginPro, version 7.5), as shown in **Figure 1**. In addition, average RGB intensity values from fruit images were obtained using the color histogram tool of Image J (National Institutes of Health, Bethesda, MD).

ANN Model. ANN, the structure and function of which are inspired by the organization and function of the human brain (*49*), is a nonlinear mathematical model that has the capability of developing meaningful relationships between input and output variables through a learning process. Many theoretical works have shown that a single hidden layer is sufficient for ANN to approximate any complex nonlinear function (*50*). Therefore, a one-hidden-layer feed-forward network structure with input, output, and hidden layers was used in this study. **Figure 2** gives a diagrammatic representation of an ANN containing multi-input neurons (**A**, 15 fractal parameters; **B**, 3 RGB intensity values) and one output neuron (for AC, AA, TP, TF, or SA). In this study, the number of neurons within the hidden layer varied from 1 to 10. The back-propagation algorithm was utilized in training of ANN models (*51*). The hyperbolic tangent sigmoid was used as the transfer function in the hidden layer and output layer. Minimization of error was accomplished using the Levenberg−Marquardt (LM) algorithm (*52*, *53*). The numerical values of the input and output variables were normalized in the range of 0−1.

Training was based on a supervised method with back-propagation strategy and was finished when the mean square error (MSE) converged and was <0.01. If the MSE did not go below 0.01, training was completed after 1000 epochs, where an epoch represents one complete sweep through all of the data in the training set. This ANN was designed and programmed by Matlab R2010a.

PLSR Model. PLSR is a linear algorithm for modeling the relationship between two data sets (*27*). In this study, all fractal parameters and individual quality indicators (AC, AA, TP, TF, or SA) were used to form the explanatory matrix (X) and dependent matrix (Y), respectively. PLSR was performed for the explanatory matrix (X) and dependent matrix (Y) to study the regression model, which showed the relationship between fractal parameters and chemical constituents during storage of bayberry juice. The number of PLSR components to be included in the analysis was determined by cross-validation (*54*), which is based on the number of PLSR components with the smallest prediction error. The PLSR was performed using SAS software (SAS, version 8.1).

Models Evaluation. To assess model performance and handle overfitting, a Monte Carlo technique (*55*) was used for cross-validation of the ANN and PLSR models in this study, described as follows: (i) the original data set of 40 samples was randomly divided into two subsets in a 7:3 ratio,

Table 1. Fractal Parameters; Red, Green, and Blue Intensity Values; and Nutrition Parameters Used for ANN and PLSR Models in This Study

parameter	no. of samples	range (min−max)	mean
fractal parameters			
red			
X_a	40	93.39−182.43	146.15
X_b	40	108.06−196.49	160.29
X	40	100.00−189.00	152.63
Y	40	1.55−1.84	1.73
S	40	4.81−9.10	6.78
green			
X_a	40	0.47−93.39	35.14
X_b	40	8.01−111.11	51.00
X	40	3.00−101.00	41.46
Y	40	1.55−1.80	1.70
S	40	3.35−11.61	7.36
blue			
X_a	40	0.47−67.10	18.47
X_b	40	4.95−88.09	35.90
X	40	3.00−75.00	24.51
Y	40	1.50−1.77	1.66
S	40	1.70−14.10	7.89
color intensity parameters			
R	40	110.24−188.51	153.82
G	40	3.33−100.91	42.86
B	40	0.84−76.25	25.83
nutrition parameters			
AC[a]	40	46.12−246.16	131.44
AA[b]	40	52.57−128.47	81.54
TP[c]	40	35.14−51.57	44.29
TF[d]	40	30.43−111.67	61.65
SA[e]	40	44.37−93.94	72.71

[a] Anthocyanin content (mg/100 mL). [b] Ascorbic acid content (mg/100 mL). [c] Total phenols content (mg/100 mL). [d] Total flavonoid content (mg/100 mL). [e] DPPH radical scavenging activity (%).

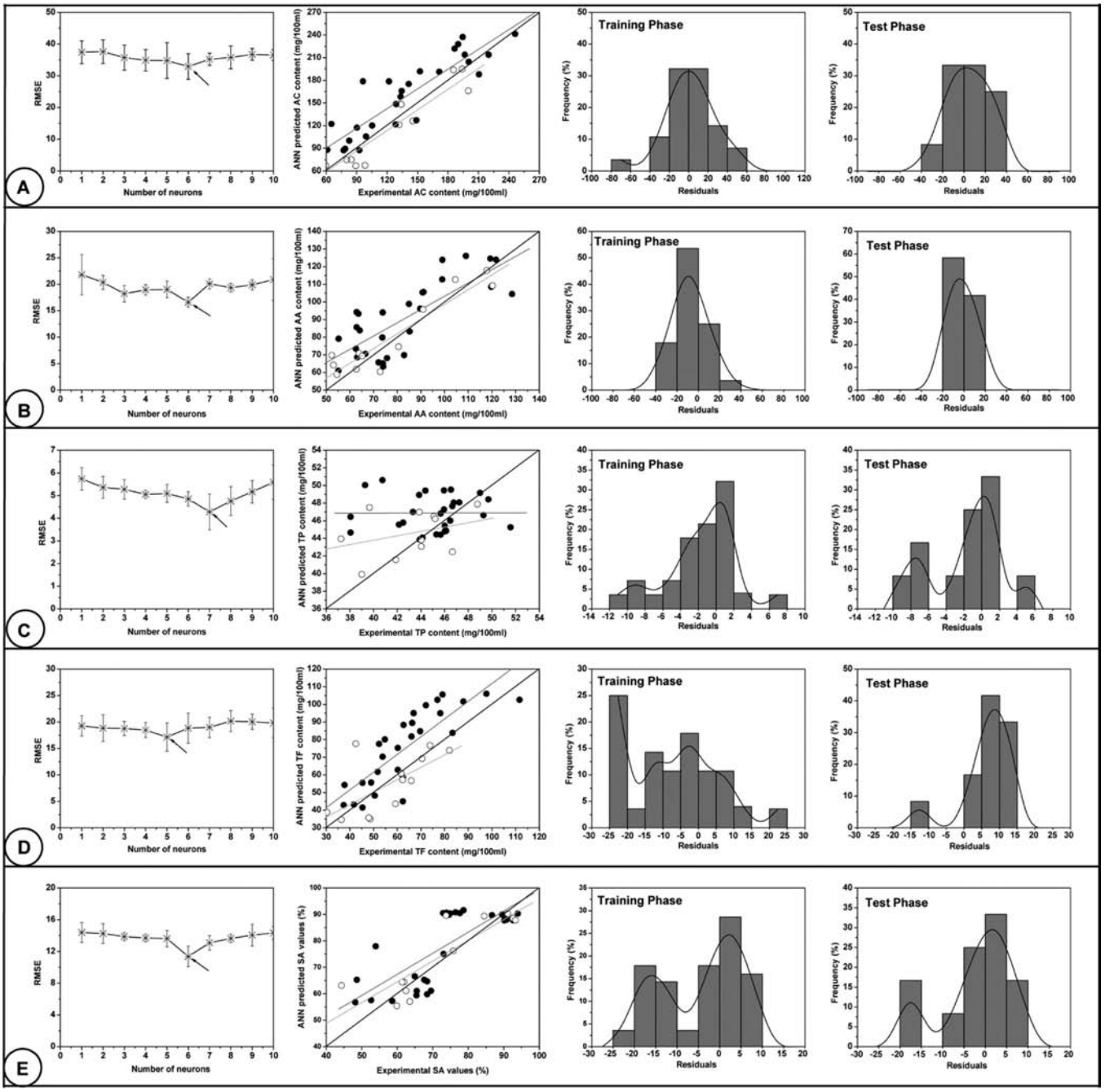

Figure 4. Parameters and performance of ANN model for predicting the change of anthocyanins (**A**), ascorbic acid (**B**), total phenols (**C**), total flavonoids (**D**), and radical DPPH scavenging activity (**E**) during storage of bayberry juice based on fractal parameters.

with 70% of the samples used for model development and the other 30% are predicted; (ii) the ANN and PLSR models were built with the training set and the root mean squared error (RMSE) calculated; (iii) steps i−iii are repeated K times ($K = 10$, in our study); (iv) the averaged RMSE was calculated, and the lower they are, the better the model. The RMSE was calculated using the equation

$$\mathrm{RMSE} = \sqrt{\frac{\sum_{i=1}^{N}(k_E - k_P)^2}{N}} \quad (2)$$

where N is the total number of data; k_P represents the predicted value from the model, whereas k_E is the experimental value.

Statistical Analysis. All determinations were carried out at least in triplicate. The data were analyzed and graphically plotted using OriginLab (OriginPro, version 7.5).

RESULTS AND DISCUSSION

Training Phase of ANN and PLSR. Figure 3 shows fractal spectra of the red, green, and blue channels derived from bayberry juice during storage. The five fractal parameters of fractal spectra of each color channel were calculated and are given in **Table 1**. Five chemical attributes (AC, AA, TP, TF, and SA) were determined for the juice samples at different storage times. **Table 1** also shows RGB intensity values and antioxidant attributes of bayberry juice. In the training phase of the ANN and PLSR models, 70% of the samples are randomly selected to build the models. To avoid overfitting, we used Monte Carlo cross-validation (*55*) to perform rigorous validations for ANN and PLSR.

The single hidden layer ANN with multi-input neurons and a single output neuron are used in this study. The optimal number of nodes in the hidden layer was selected by using a trial and error

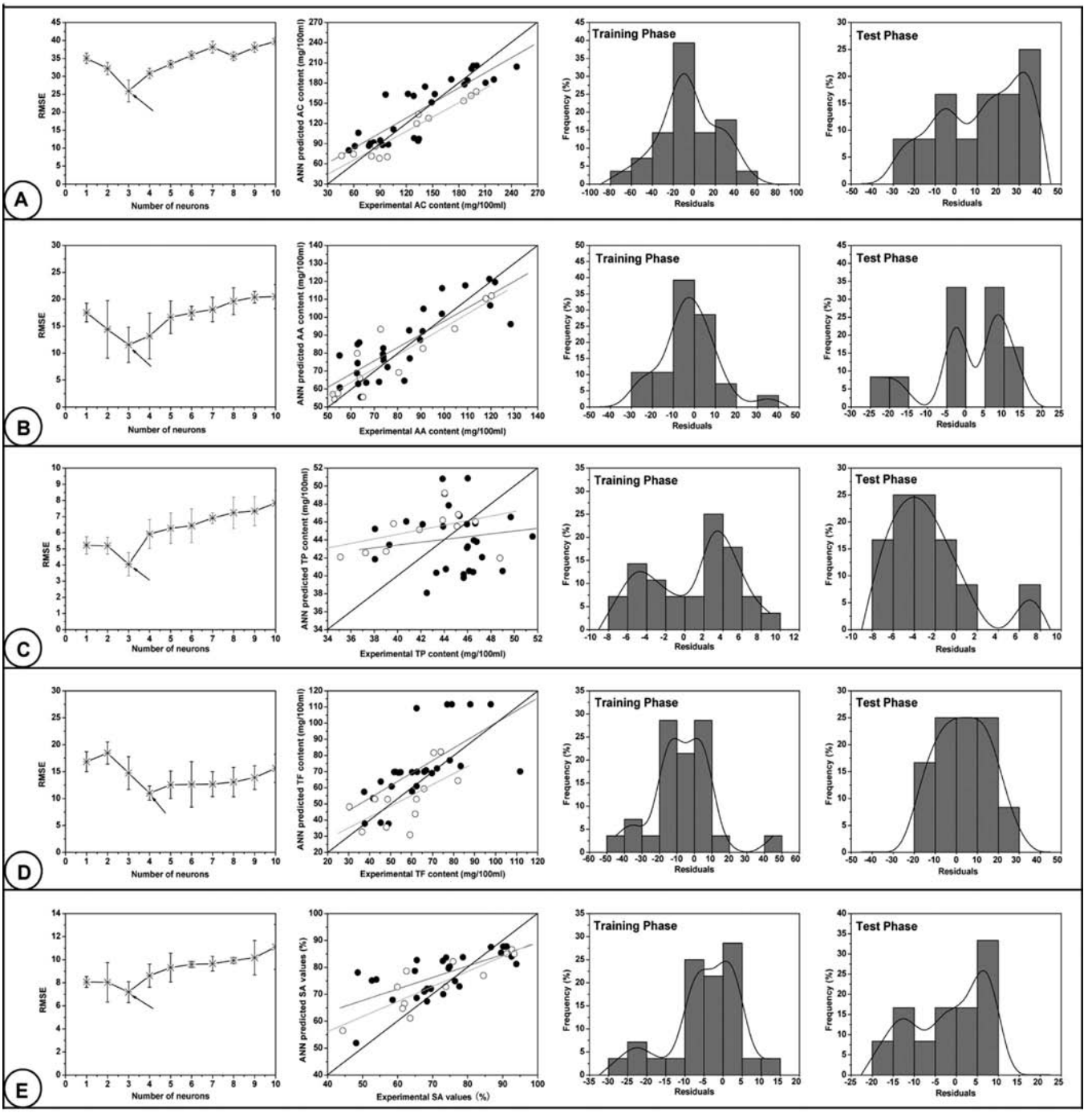

Figure 5. Parameters and performance of ANN model for predicting the change of anthocyanins (**A**), ascorbic acid (**B**), total phenols (**C**), total flavonoids (**D**), and radical DPPH scavenging activity (**E**) during storage of bayberry juice based on RGB intensity values.

method. **Figures 4** and **5** show the change of RMSE in the prediction of AC, AA, TP, TF, and SA with different numbers of neurons in the hidden layer during storage of bayberry juice based on fractal parameters and RGB intensity values, respectively. For ANN based on fractal parameters, the optimal numbers of nodes in the hidden layer are 6, 6, 7, 5, and 6 for predicting the changes of AC, AA, TP, TF, and SA, respectively. Moreover, the optimal number of nodes is 3 for AC, AA, TP, and SA and 6 for TF in the hidden layer of ANN based on RGB intensity values.

The most important linear calibration method is PLSR, because it can analyze data sets that are strongly collinear, noisy, and numerous variables (*27*). In this study, PLSR has been applied to predict the changes of AC, AA, TP, TF, and SA during storage of bayberry juice as a function of fractal parameters or RGB intensity values. In our experiment, the optimal number of PLSR model components and their predictive ability were determined using a cross-validation method. That is, to cross-validate the model with various numbers of components, choose the number with minimum prediction error on the test set and without overfitting. The RMSE of training and test phases as a function of the number of PLSR components is illustrated in **Figures 6** and **7** for PLSR models based on fractal parameters and RGB intensity values, respectively. The results show that the optimal numbers of PLSR components are 1, 1, 1, 1, and 2 for predicting the changes of AC, AA, TP, TF, and SA by PLSR

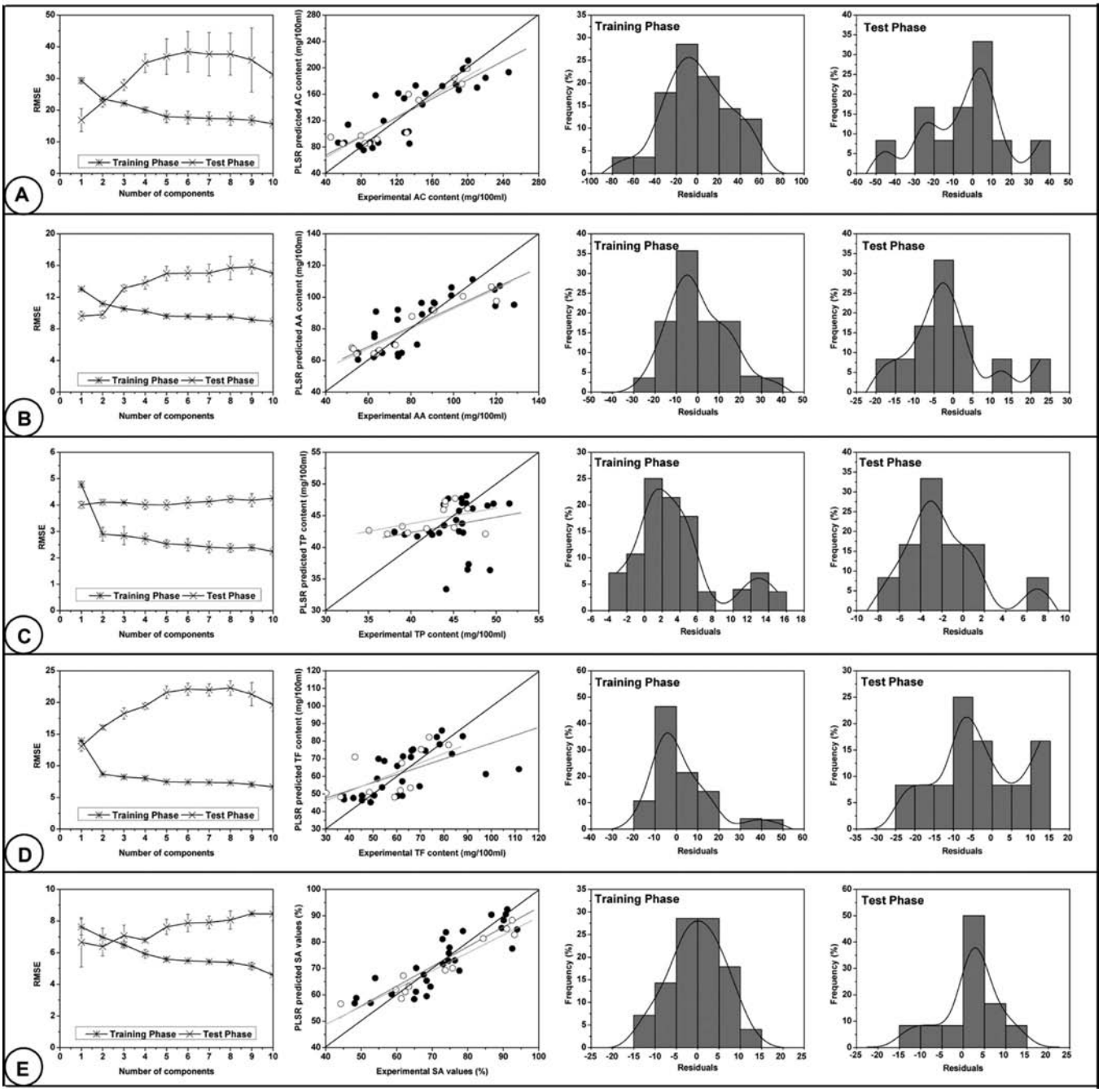

Figure 6. Parameters and performance of PLSR model for predicting the change of anthocyanins (**A**), ascorbic acid (**B**), total phenols (**C**), total flavonoids (**D**), and radical DPPH scavenging activity (**E**) during storage of bayberry juice based on fractal parameters.

based on fractal parameters, respectively. In addition, the optimal number of components in the PLSR based on RGB intensity values is 3 for prediction of all antioxidant attributes in this study.

Test Phase of ANN and PLSR. In this phase, an independent data set (30% of the total data) was utilized to test ANN and PLSR models. The agreement between the experimental data and the model-predicted values and the plot of the residual values at the stages of model evaluation are presented in **Figures 4**−**7**. The residuals from ANN based on fractal parameters for AC and AA and PLSR based on fractal parameters for SA follow the normal distribution better than others at the test phase as shown in **Figures 4**−**7**. To quantify the performance of ANN and PLSR models, various parameters between experimental and model-predicted values were calculated (**Table 2**): root-mean-square error (RMSE) and coefficient of determination (R^2). According to **Table 2**, the optimal ANN based on fractal parameters could predict the changes of AC, AA, TP, TF, and SA during storage of bayberry juice with the RMSE of 18.673 mg/100 mL, 8.694 mg/100 mL, 4.125 mg/100 mL, 13.192 mg/100 mL, and 7.957% and R^2 values of 0.939, 0.935, 0.393, 0.655 and 0.859, respectively. For ANN based on RGB intensity values, the RMSE and R^2 are 21.805 mg/100 mL and 0.923 for AC, 10.360 mg/100 mL and 0.901 for AA, 4.530 mg/100 mL and 0.409 for TP, 14.128 mg/100 mL and 0.624 for TF, and 8.421% and 0.869 for SA, respectively. The PLSR model for predicting the changes of AC, AA, TP, TF, and SA has RMSE values of 20.975 mg/100 mL, 10.265 mg/100 mL, 3.914 mg/100 mL, 12.521 mg/100 mL, and 5.966% and the R^2 values of 0.918, 0.943, 0.455, 0.641, and 0.958 based on fractal parameters and RMSE values of 19.140 mg/100 mL, 9.930 mg/100 mL, 3.860 mg/100 mL, 12.790 mg/100 mL, and 6.780% and the

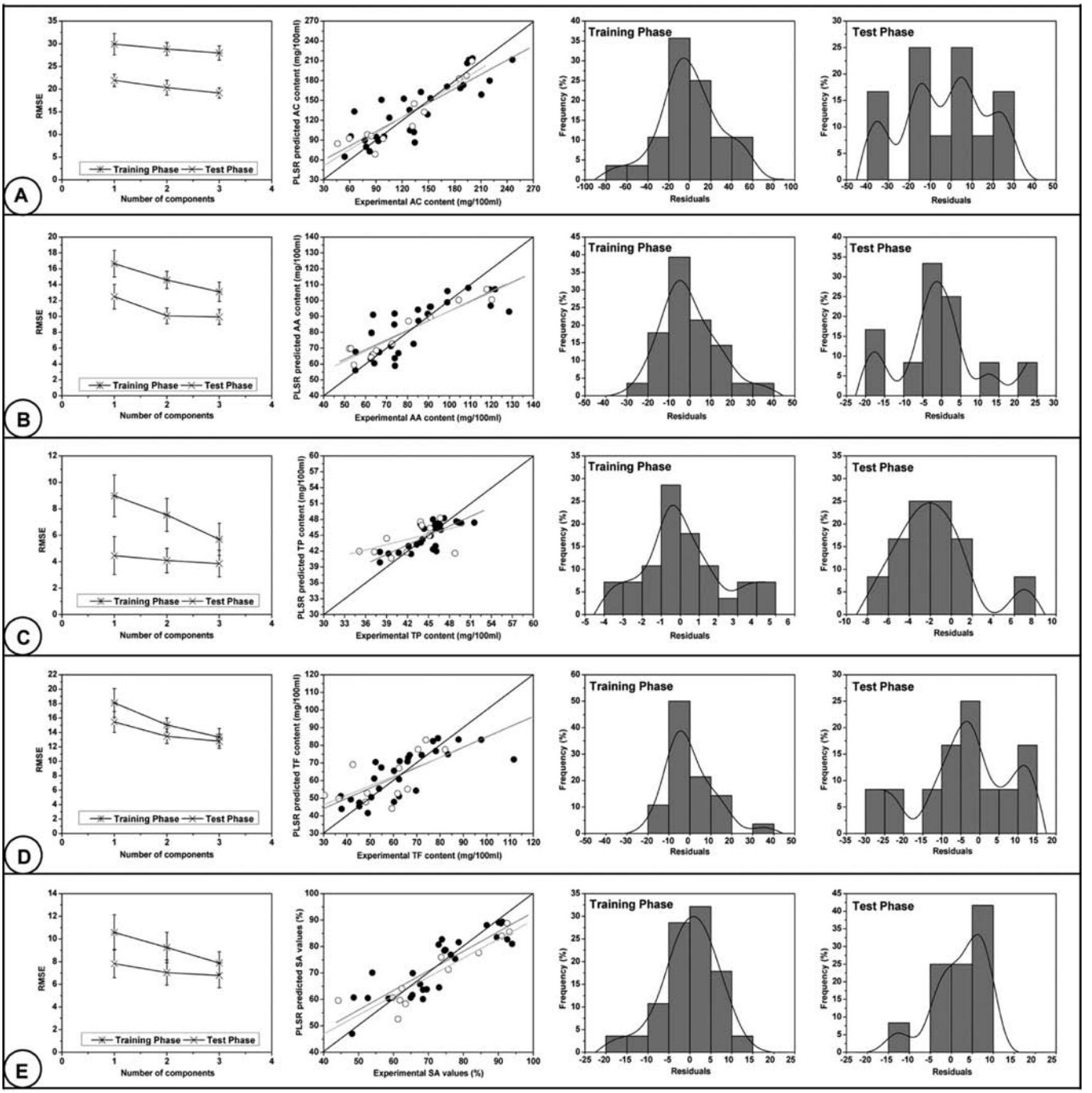

Figure 7. Parameters and performance of PLSR model for predicting the change of anthocyanins (**A**), ascorbic acid (**B**), total phenols (**C**), total flavonoids (**D**), and radical DPPH scavenging activity (**E**) during storage of bayberry juice based on RGB intensity values.

R^2 of 0.931, 0.953, 0.489, 0.630, and 0.915 based on RGB intensity values, respectively. For the prediction of AC and AA, the R^2 of all prediction methods is >0.9, but the RMSE of ANN based on fractal parameters is lower than that of other methods. According to **Table 2**, the prediction error (RMSE) of ANN based on fractal parameters could decrease 2.44 and 12.45% for AC and AA compared with PLSR based on RGB intensity values, respectively. Thus, ANN model combined with fractal analysis is recommended for application in the prediction of changes in AC and AA during storage of bayberry juice in this study. For the prediction of SA, the PLSR model can be considered satisfactory, because the R^2 values are >0.9. The PLSR based on fractal parameters, however, has lower RMSE and higher R^2 than the PLSR based on RGB intensity values. From **Table 2**, the prediction error decreased by 12.01% for SA using PLSR based on fractal parameters. In this study, the poor R^2 values ($R^2 = 0.624$ and 0.655 for ANN and $R^2 = 0.630$ and 0.641 for PLSR) indicate that the ANN and PLSR models have poor performances for the prediction of TF during storage of bayberry juice based on fractal parameters and RGB intensity values. In addition, all methods for predicting the change of TP provide low R^2 values ($R^2 = 0.393$ and 0.409 for ANN and $R^2 = 0.455$ and 0.498 for PLSR), which indicate a poor relationship between the degradation of TP and the changes of fractal parameters and RGB intensity values during storage of bayberry juice. One possible explanation for these results is that TP content in bayberry juice is more stable than its color during storage. Our data show the change of TP content during the 12 day storage period at 25 °C ranged from 35.14 to 51.57 mg/100 mL juice. Other papers

Table 2. Root Mean Squared Errors (RMSE) and Coefficients of Determination (R^2) in the Prediction of the Changes of Nutritional Components during Storage of Bayberry Juice at the Test Phases by ANN and PLSR Models Based on Fractal Parameters and RGB Intensity Values

	fractal parameters				RGB intensity values			
	ANN		PLSR		ANN		PLSR	
	RMSE[f]	R^2	RMSE	R^2	RMSE	R^2	RMSE	R^2
AC[a]	18.673	0.939	20.975	0.918	21.805	0.923	19.140	0.931
AA[b]	8.694	0.935	10.265	0.943	10.360	0.901	9.930	0.953
TP[c]	4.125	0.393	3.914	0.455	4.530	0.409	3.860	0.498
TF[d]	13.192	0.655	12.521	0.641	14.128	0.624	12.790	0.630
SA[e]	7.957	0.859	5.966	0.958	8.421	0.869	6.780	0.915

[a] Anthocyanin content (mg/100 mL). [b] Ascorbic acid content (mg/100 mL). [c] Total phenols content (mg/100 mL). [d] Total flavonoid content (mg/100 mL). [e] DPPH radical scavenging activity (%). [f] mg/100 mL or %.

have also shown the total phenol concentration in apples to be relatively stable during storage (*56*).

In conclusion, the ANN model combined with fractal analysis as a potential tool can be used to predict the changes of AC and AA in bayberry juice during storage, and the PLSR model based on fractal parameters is adequate for the prediction of SA in this study. However, both models have poor performances for estimating the change of TP and TF during storage of bayberry juice based on fractal parameters and RGB intensity values. The success of this research will present a new method for quality evaluation of bayberry juice during processing, storage, and distribution. It is, however, of great importance to select the most adequate model for the evaluation of different nutritional components in bayberry juice.

ABBREVIATIONS USED

ANN, artificial neural network; PLSR, partial least-squares regression; AC, anthocyanin; AA, ascorbic acid; TP, total phenols; TF, total flavonoid; SA, DPPH radical scavenging activity.

ACKNOWLEDGMENT

We thank Dr. Oldrich Zmeskal, Tomas Bzatek, and Martin Nezadal from Brno University of Technology (Czech Republic) for supplying HarFA 5.4 software. We also sincerely thank Associate Prof. Zhonglong Zheng in the College of Information Science and Engineering at Zhejiang Normal University (Jinhua, China) for his assistance with the revision of the manuscript.

LITERATURE CITED

(1) Chen, K. S.; Xu, C. J.; Zhang, B. Red bayberry: botany and horticulture. *Hortic. Rev.* **2004**, *30*, 83−114.

(2) Li, X.; He, Y. Non-destructive measurement of acidity of Chinese bayberry using VIS/NIRS techniques. *Eur. Food Res. Technol.* **2006**, *223* (6), 731−736.

(3) Xi, Y. F.; Zheng, Y. H. Effect of temperature on the nutrients and rot of bayberry during post-harvesting. *Bull. Sci. Technol.* **1993**, *9*, 254−256.

(4) Wang, K.; Jin, P.; Cao, S.; Shang, H.; Yang, Z.; Zheng, Y. Methyl jasmonate reduces decay and enhances antioxidant capacity in Chinese bayberries. *J. Agric. Food Chem.* **2009**, *57*, 5809−5815.

(5) Yang, Z.; Zheng, Y.; Cao, S. Effect of high oxygen atmosphere storage on quality, antioxidant enzymes, and DPPH-radical scavenging activity of Chinese bayberry fruit. *J. Agric. Food Chem.* **2009**, *57*, 176−181.

(6) Cemeroglu, B.; Velioglu, S.; Isik, S. Degradation kinetics of anthocyanins in sour cherry juice and concentrate. *J. Food Sci.* **1994**, *59*, 1216−1218.

(7) Alighourchi, H.; Barzegar, M. Some physicochemical characteristics and degradation kinetic of anthocyanin of reconstituted pomegranate juice during storage. *J. Food Eng.* **2009**, *90*, 179−185.

(8) Burdurlu, H. S.; Koca, N.; Karadeniz, F. Degradation of vitamin C in citrus juice concentrates during storage. *J. Food Eng.* **2006**, *74*, 211−216.

(9) Al-Zubaidy, M. M. I.; Khalil, R. A. Kinetic and prediction studies of ascorbic acid degradation in normal and concentrate local lemon juice during storage. *Food Chem.* **2007**, *101*, 254−259.

(10) Sharma, S. K.; Maguer, M. L. Kinetics of lycopene degradation in tomato pulp solids under different processing and storage conditions. *Food Res. Int.* **1996**, *29*, 309−315.

(11) Manso, M. C.; Oliveira, F. A. R.; Oliveira, J. C.; Frías, J. M. Modelling ascorbic acid thermal degradation and browning in orange juice under aerobic conditions. *Int. J. Food Sci. Technol.* **2001**, *36* (3), 303−312.

(12) Oms-Oliu, G.; Odriozola-Serrano, I.; Soliva-Fortuny, R.; Martín-Belloso, O. Use of Weibull distribution for describing kinetics of antioxidant potential changes in fresh-cut watermelon. *J. Food Eng.* **2009**, *95*, 99−105.

(13) Odriozola-Serrano, I.; Soliva-Fortuny, R.; Martín-Belloso, O. Influence of storage temperature on the kinetics of the changes in anthocyanins, vitamin C, and antioxidant capacity in fresh-cut strawberries stored under high-oxygen atmospheres. *J. Food Sci.* **2009**, *2* (74), 184−191.

(14) Singh, R. P.; Heldman, D. R. Simulation of liquid food quality during storage. *Trans. ASAE* **1976**, *19* (1), 178−184.

(15) Lee, Y. C.; Kirk, J. R.; Bedford, C. L.; Heldman, D. R. Kinetics and computer simulation of ascorbic acid stability of tomato juice as function of temperature, pH and metal catalyst. *J. Food Sci.* **1977**, *3* (42), 640−643.

(16) Guillard, V.; Broyart, B.; Bonazzi, C.; Guilbert, S.; Gontard, N. Evolution of moisture distribution during storage in a composite food modelling and simulation. *J. Food Sci.* **2003**, *68*, 958−966.

(17) Maier, H. R.; Dandy, G. C. Neural network based modelling of environmental variables: a systematic approach. *Math. Comput. Model.* **2001**, *33*, 669−682.

(18) Kaastra, I.; Boyd, M. Designing a neural network for forecasting financial and economic time series. *Neurocomputing* **1996**, *10*, 215−236.

(19) Fang, Y. C.; Wu, B. W. Neural network application for thermal image recognition on flow-resolution objects. *J. Opt. A: Pure Appl. Opt.* **2007**, *9* (2), 134−144.

(20) Parlak, A.; Islamoglu, Y.; Yasar, H.; Egrisogut, A. Application of artificial neural network to predict specific fuel consumption and exhaust temperature for a diesel engine. *Appl. Therm. Eng.* **2006**, *26*, 824−828.

(21) Yuanyou, X; Yanming, X; Ruigeng, Z. An engineering geology evaluation method based on an artificial neural network and its application. *Eng. Geol.* **1997**, *47* (1−2), 149−156.

(22) Maier, H. R; Dandy, G. C. Neural networks for the prediction and forecasting water resources variables: a review of modeling issues and applications. *Environ. Model Soft.* **2000**, *15*, 101−124.

(23) Buciński, A.; Zieliński, H.; Kozłowska, H. Artificial neural networks for prediction of antioxidant capacity of cruciferous sprouts. *Trends Food Sci. Technol.* **2004**, *15*, 161−169.

(24) Tripathy, P. P.; Kumar, S. Neural network approach for food temperature prediction during solar drying. *Int. J. Therm. Sci.* **2009**, *48*, 1452−1459.

(25) Lu, H. F.; Zheng, H.; Lou, H. Q.; Jiang, L. L.; Chen, Y.; Fang, S. S. Using neural networks to estimate the losses of ascorbic acid, total phenols, flavonoid, and antioxidant activity in asparagus during thermal treatments. *J. Agric. Food Chem.* **2010**, *58*, 2995−3001.
(26) Goñi, S. M.; Oddone, S.; Segura, J. A.; Mascheroni, R. H.; Salvadori, V. O. Prediction of foods freezing and thawing times: Artificial neural networks and genetic algorithm approach. *J. Food Eng.* **2008**, *84*, 164−178.
(27) Wold, S.; Trygg, J.; Berglund, A.; Antti, H. Some recent developments in PLS modelling. *Chemom. Intell. Lab. Sys.* **2001**, *58*, 131−150.
(28) Roy, K.; Roy, P. P. Comparative chemometric modeling of cytochrome 3A4 inhibitory activity of structurally diverse compounds using stepwise MLR, FA-MLR, PLS, GFA, G/PLS and ANN techniques. *Eur. J. Med. Chem.* **2009**, *44*, 2913−2922.
(29) Adhikari, N.; Maiti, M. K.; Jha, T. Predictive comparative QSAR modelling of (phenylpiperazinyl-alkyl) oxindoles as selective 5-HT_{1A} antagonists by stepwise regression, PCRA, FA-MLR and PLS techniques. *Eur. J. Med. Chem.* **2010**, *45*, 1119−1127.
(30) Ramírez, J.; Górriz, J. M.; Segovia, F.; Chaves, R.; Salas-Gonzalez, D.; López, M.; Álvarez, I.; Padilla, P. Computer aided diagnosis system for the Alzheimer's disease based on partial least squares and random forest SPECT image classification. *Neurosci. Lett.* **2010**, *472*, 99−103.
(31) Niu, X. Y.; Shen, F.; Yu, Y. F.; Yan, Z. K.; Xu, K.; Yu, H. Y.; Ying, Y. B. Analysis of sugars in Chinese rice wine by fourier transform near-infrared spectroscopy with partial least-squares regression. *J. Agric. Food Chem.* **2008**, *56*, 7271−7278.
(32) Association of the Industry of Juices and Nectars from Fruits and Vegetables (AIJN). *Association of the Industry of Juices and Nectars of the European Economic Community Code of Practice for Evaluation of Fruit and Vegetable Juices*; AIJN: Brussels, Belgium, 1996.
(33) Tepper, B. J. Effects of a slight color variation on consumer acceptance of orange juice. *J. Sensory Stud.* **1993**, *8*, 145−154.
(34) Walkowiak-Tomczak, D.; Czapski, J. Colour changes of a preparation from red cabbage during storage in a model system. *Food Chem.* **2007**, *104*, 709−714.
(35) Niamnuy, C.; Devahastin, S.; Soponronnarit, S.; Raghavan, V. G. S. Kinetics of astaxanthin degradation and color changes of dried shrimp during storage. *J. Food Eng.* **2008**, *87*, 591−600.
(36) Gonçalves, E. M.; Cruz, R. M. S.; Abreu, M.; Brandão, T. R. S.; Silva, C. L. M. Biochemical and colour changes of watercress (*Nasturtium officinale* R. Br.) during freezing and frozen storage. *J. Food Eng.* **2009**, *93*, 32−39.
(37) Mandelbrot, B. B. *Fractal Geometry of Nature*; Freeman Press: San Francisco, CA, 1982.
(38) Pandolfi, C.; Messina, G.; Mugnai, S.; Azzarello, E.; Masi, E.; Dixon, K.; Mancuso, S. Discrimination and identification of morphotypes of *Banksia integrifolia* (Proteaceae) by an artificial neural network (ANN) based on morphological and fractal parameters of leaves and flowers. *TAXON* **2009**, *58* (3), 925−933.
(39) Chen, C. C.; Daponte, J. S.; Fox, M. D. Fractal feature analysis and classification in medical imaging. *IEEE Trans. Med. Imag.* **1989**, *6*, 133−142.
(40) Wu, C. M.; Chen, Y. C.; Hsieh, K. S. Texture features for classification of ultrasonic liver images. *IEEE Trans. Med. Imag.* **1992**, *11*, 141−152.
(41) Liu, D.; Zhao, K.; Zou, H.; Su, J. Fractal analysis with applications to seismological pattern recognition of underground nuclear explosion. *Signal Process* **2000**, *80*, 1849−1861.
(42) He, Z.; You, X.; Yuan, Y. Texture image retrieval based on non-tensor product wavelet filter banks. *Signal Process* **2009**, *89*, 1501−1510.
(43) Barrett, A. H.; Peleg, M. Applications of fractal analysis to food structure. *LWT−Food Sci. Technol.* **1995**, *28*, 553−563.
(44) Meyers, K. J.; Watkins, C. B.; Pritts, M. P.; Liu, R. H. Antioxidant and antiproliferative activities of strawberries. *J. Agric. Food Chem.* **2003**, *51*, 6887−6892.
(45) Bao, J. S.; Cai, Y. Z.; Sun, M.; Wang, G. Y.; Corke, H. Anthocyanins, flavonols and free radical scavenging activity of Chinese bayberry (*Myrica rubra*) extracts and their colour properties and stability. *J. Agric. Food Chem.* **2005**, *53*, 2327−2332.
(46) Alasalvar, C.; Al-Farsi, M.; Quantick, P. C.; Shahidi, F.; Wiktorowicz, R. Effect of chill storage and modified atmosphere packaging (MAP) on antioxidant activity, anthocyanins, carotenoids, phenolics and sensory quality of ready-to-eat shredded orange and purple carrots. *Food Chem.* **2005**, *89* (1), 69−76.
(47) Giusti, M. M.; Wrolstad, R. E. Unit F1.2. Anthocyanins. Characterization and measurement with UV−visible spectroscopy. In *Current Protocols in Food Analytical Chemistry*; Wrolstad, R. E., Schwartz, S. J., Eds.; Wiley: New York, 2001; pp 1−13.
(48) Zheng, H.; Lu, H.; Zheng, Y.; Lou, H.; Chen, C. Automatic sorting of Chinese jujube (*Zizyphus jujuba* Mill. cv. 'hongxing') using chlorophyll fluorescence and support vector machine. *J. Food Eng.* **2010**, *101*, 402−408.
(49) Bila, S.; Harkouss, Y.; Ibrahim, M.; Rousset, J.; N'Goya, E.; Baillargeat, D.; Verdeyme, S.; Aubourg, M.; Guillon, P. An accurate wavelet neural-network-based model for electromagnetic optimization of microwave circuits. *Int. J. RF Microwave CAE* **1999**, *93*, 297−306.
(50) Dogan, A.; Demirpence, H.; Cobaner, M. Prediction of groundwater levels from lake levels and climate data using ANN approach. *Water SA* **2008**, *34* (2), 1−10.
(51) Hornik, K.; Stinchombe, M.; White, H. Multilayer feed forward network are universal approximator. *Neural Network* **1989**, *2*, 359−366.
(52) Levenberg, K. A method for the solution of certain non-linear problems in least squares. *Q. J. Appl. Math.* **1944**, *2* (2), 164−168.
(53) Marquardt, D. W. An algorithm for least-squares estimation of nonlinear parameters. *J. Soc. Ind. Appl. Math.* **1963**, *2* (2), 431−441.
(54) Martens, M.; Martens, H. *Statistical Procedure in Food Research*' Elsevier Applied Science: London, U.K., 1986.
(55) Xu, Q. S.; Liang, Y. Z.; Du, Y. P. Monte Carlo cross-validation for selecting a model and estimating the prediction error in multivariate calibration. *J. Chemom.* **2004**, *18*, 112−120.
(56) Coseteng, M. Y.; Lee, C. Y. Changes in apple polyphenoloxidase and polyphenol concentrations in relation to degree of browning. *J. Food Sci.* **1987**, *52*, 985−989.

Received for review August 20, 2010. Revised manuscript received November 26, 2010. Accepted December 10, 2010. We thank the Postgraduate Innovation Research Projects of Zhejiang Province (YK2008038) for partially funding this study.